

Properties of tunnel Josephson junctions with a ferromagnetic interlayer

A. S. Vasenko,^{1,2,*} A. A. Golubov,¹ M. Yu. Kupriyanov,³ and M. Weides⁴

¹*Faculty of Science and Technology and MESA⁺ Institute for Nanotechnology, University of Twente, 7500 AE Enschede, The Netherlands*

²*Department of Physics, Moscow State University, Moscow 119992, Russia*

³*Nuclear Physics Institute, Moscow State University, Moscow 119992, Russia*

⁴*Center of Nanoelectronic Systems for Information Technology (CNI), Research Centre Jülich, D-52425 Jülich, Germany*

(Received 31 October 2007; revised manuscript received 17 December 2007; published 4 April 2008)

We investigate superconductor/insulator/ferromagnet/superconductor tunnel Josephson junctions in the dirty limit using the quasiclassical theory. We formulate a quantitative model describing the oscillations of critical current as a function of thickness of the ferromagnetic layer and use this model to fit recent experimental data. We also calculate quantitatively the density of states (DOS) in this type of junctions and compare DOS oscillations with those of the critical current.

DOI: [10.1103/PhysRevB.77.134507](https://doi.org/10.1103/PhysRevB.77.134507)

PACS number(s): 74.50.+r, 74.45.+c, 74.78.Fk, 75.30.Et

I. INTRODUCTION

It is well known that superconductivity and ferromagnetism are two competing orders; however, their interplay can be realized when the two interactions are spatially separated. In this case, the coexistence of the two orderings is due to the proximity effect.¹⁻³ Experimentally, this situation can be realized in superconductor/ferromagnet (S/F) hybrid structures. The main manifestation of the proximity effect in S/F structures is the damped oscillatory behavior of the superconducting correlations in the F layers. Two characteristic lengths of the decay and oscillations are, correspondingly, ξ_{f1} and ξ_{f2} . Unusual proximity effect in S/F layered structures leads to a number of striking phenomena such as nonmonotonic dependence of their critical temperature and oscillations of critical current in S/F/S Josephson junctions upon the F layer thickness. Negative sign of the critical current corresponds to the so-called π state. Spontaneous π phase shifts in S/F/S junctions were observed experimentally.⁴⁻¹⁵

Superconductor / insulator / ferromagnet / superconductor (SIFS) junctions, i.e., S/F/S trilayers with one transparent interface and one tunnel barrier between S and F layers, represent practically interesting case of π junctions. SIFS structure offers the freedom to tune the critical current density over a wide range and at the same time to realize high values of a product of the junction critical current I_c and its normal state resistance R_N .^{14,15} In addition, Nb based tunnel junctions are usually underdamped, which is desired for many applications. SIFS π junctions have been proposed as potential logic elements in superconducting logic circuits.¹⁶ SIFS junctions are also interesting from the fundamental point of view since they provide a convenient model system for a comparative study between 0- π transitions observed from the critical current and from the density of states (DOS). At the same time, despite such an interest, there is no complete theory yet of SIFS junctions which could provide quantitative predictions for critical current and DOS in such structures. All existing theories dealt only with a number of limiting cases, when either linearized quasiclassical equations can be used for analysis¹⁷ (e.g., temperature range near critical temperature, small transparency of interfaces) or thickness of the F layer is small¹⁻³ compared to the decay char-

acteristic length ξ_{f1} . Further, in symmetric S/F/S junctions, the extension of theory to the case of nonhomogeneous magnetization and large mean free path was performed in Refs. 3 and 18.

The purpose of this work is to provide a quantitative model describing the behavior of critical current and DOS in SIFS junctions as a function of parameters characterizing material properties of the S and F layers and the S/F interface transparency. The model provides a tool to fit experimental data in existing SIFS junctions.

The paper is organized as follows. In the next section, we formulate the theoretical model and basic equations. In Sec. III, we solve nonlinear Usadel equations, apply solutions for calculation of critical current in SIFS junctions with long ferromagnetic layer, $d_f \gg \xi_{f1}$, and fit recent experimental data. In Sec. IV, we perform numerical calculations for critical current in a SIFS junction with arbitrary length of the F layer. In Sec. V, we numerically calculate DOS in the ferromagnetic interlayer, and then summarize results in Sec. VI.

II. MODEL AND BASIC EQUATIONS

The model of an S/F/S junction we are going to study is depicted in Fig. 1 and consists of a ferromagnetic layer of thickness d_f and two thick superconducting electrodes along the x direction. Left and right superconductor/ferromagnet interfaces are characterized by the dimensionless parameters γ_{B1} and γ_{B2} , respectively, where $\gamma_{B1,B2} = R_{B1,B2} \sigma_n / \xi_n$, $R_{B1,B2}$ are the resistances of left and right S/F interfaces, respectively, σ_n is the conductivity of the F layer, $\xi_n = \sqrt{D_f / 2\pi T_c}$,

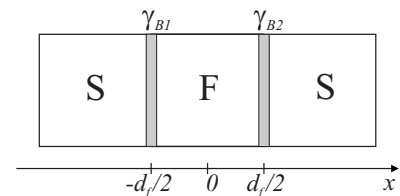


FIG. 1. Geometry of the considered system. The thickness of the ferromagnetic interlayer is d_f . The transparency of the left S/F interface is characterized by the γ_{B1} coefficient, and the transparency of the right F/S interface is characterized by γ_{B2} .

D_f is the diffusion coefficient in the ferromagnetic metal, and T_c is the critical temperature of the superconductor (we assume $\hbar = k_B = 1$). We also assume that the S/F interfaces are not magnetically active. We will consider diffusive limit, in which the elastic scattering length ℓ is much smaller than the decay characteristic length ξ_{f1} . In this paper we concentrate on the case of a SIFS tunnel Josephson junction, when $\gamma_{B1} \gg 1$ (tunnel barrier) and $\gamma_{B2} = 0$ (fully transparent interface). For comparison, we also consider two other limiting cases: an SFS junction ($\gamma_{B1} = \gamma_{B2} = 0$) and a SIFIS junction ($\gamma_{B1}, \gamma_{B2} \gg 1$).

Under conditions described above, the calculation of the Josephson current requires solution of the one-dimensional Usadel equations.¹⁹ In the F layer, the equation has the form^{20,21}

$$D_f \frac{\partial}{\partial x} \left(\hat{G}_{f\uparrow(\downarrow)} \frac{\partial}{\partial x} \hat{G}_{f\uparrow(\downarrow)} \right) = \left[(\omega \pm ih) \sigma_z + \frac{1}{2\tau_m} \sigma_z \hat{G}_{f\uparrow(\downarrow)} \sigma_z \hat{G}_{f\uparrow(\downarrow)} \right], \quad (1)$$

where positive sign ahead of h corresponds to the spin up state (\uparrow) and negative sign to the spin down state (\downarrow), $\omega = 2\pi T(n + \frac{1}{2})$ are the Matsubara frequencies, h is the exchange field in the ferromagnet, and σ_z is the Pauli matrix in the Nambu space. The parameter τ_m is the spin-flip scattering time. The influence of spin-flip scattering on various properties of S/F structures was considered in a number of papers.^{13,20–22,25,31,32} We consider the ferromagnet with strong uniaxial anisotropy, in which case the magnetic scattering does not couple the spin up and spin down electron populations.

The Usadel equation in the S layer can be written as¹⁹

$$D_s \frac{\partial}{\partial x} \left(\hat{G}_s \frac{\partial}{\partial x} \hat{G}_s \right) = [\omega \sigma_z + \hat{\Delta}(x), \hat{G}_s], \quad (2)$$

where D_s is the diffusion coefficient in the superconductor. In Eq. (2), $\hat{G}_s \equiv \hat{G}_{s\uparrow(\downarrow)}$ and we omit subscripts “ \uparrow (\downarrow)” because equations in superconductor look identically for spin up and spin down electron states.

In Eqs. (1) and (2), we use following matrix notations (we omit f , s , and \uparrow (\downarrow) subscripts):

$$\hat{G}(x, \omega) = \begin{pmatrix} G & F \\ F^* & -G \end{pmatrix}, \quad \hat{\Delta}(x) = \begin{pmatrix} 0 & \Delta(x) \\ \Delta^*(x) & 0 \end{pmatrix}, \quad (3)$$

where G and F are normal and anomalous Green’s functions, respectively, and $\Delta(x)$ is the superconducting pair potential. The matrix Green’s function \hat{G} satisfies the normalization condition

$$\hat{G}^2 = 1, \quad G^2 + FF^* = 1, \quad (4)$$

and the pair potential $\Delta(x)$ is determined by the self-consistency equation,

$$\Delta(x) \ln \frac{T_c}{T} = \pi T \sum_{\omega > 0} \left(\frac{2\Delta(x)}{\omega} - F_{s\uparrow} - F_{s\downarrow} \right). \quad (5)$$

The boundary conditions for the Usadel equations at the left and right sides of each S/F interface are given by relations²³

$$\xi_n \gamma \left(\hat{G}_f \frac{\partial}{\partial x} \hat{G}_f \right)_{\pm d_f/2} = \xi_s \left(\hat{G}_s \frac{\partial}{\partial x} \hat{G}_s \right)_{\pm d_f/2}, \quad (6a)$$

$$2\xi_n \gamma_{B1} \left(\hat{G}_f \frac{\partial}{\partial x} \hat{G}_f \right)_{-d_f/2} = [\hat{G}_s, \hat{G}_f]_{-d_f/2}, \quad (6b)$$

$$2\xi_n \gamma_{B2} \left(\hat{G}_f \frac{\partial}{\partial x} \hat{G}_f \right)_{d_f/2} = [\hat{G}_f, \hat{G}_s]_{d_f/2}, \quad (6c)$$

where $\gamma = \xi_s \sigma_n / \xi_n \sigma_s$, σ_s is the conductivity of the S layer, and $\xi_s = \sqrt{D_s / 2\pi T_c}$.

To complete the boundary problem, we also set boundary conditions at $x = \pm \infty$,

$$G_s(\pm \infty) = \frac{\omega}{\sqrt{|\Delta|^2 + \omega^2}}, \quad (7a)$$

$$F_s(-\infty) = \frac{|\Delta| e^{-i\varphi/2}}{\sqrt{|\Delta|^2 + \omega^2}}, \quad F_s(+\infty) = \frac{|\Delta| e^{i\varphi/2}}{\sqrt{|\Delta|^2 + \omega^2}}, \quad (7b)$$

where φ is the superconducting phase difference between S electrodes.

In Matsubara technique, it is convenient to parametrize the Green’s function in the following way, making use of the normalization condition [Eq. (4)].²⁴

$$\hat{G} = \begin{pmatrix} \cos \theta & \sin \theta e^{i\chi} \\ \sin \theta e^{-i\chi} & -\cos \theta \end{pmatrix}. \quad (8)$$

Solving a system of nonlinear differential equations [Eqs. (1)–(7)], generally can be fulfilled only numerically. We present full numerical calculation in Sec. IV. The analytical solution can be constructed in case of one S/F bilayer, when we can set the phase χ in Eq. (8) to zero. We can also set the phase to zero in case of long S/F/S junction, where the thickness of the ferromagnetic layer $d_f \gg \xi_{f1}$. In that case, the decay of the Cooper pair wave function in first approximation occurs independently near each interface. Therefore, we can consider the behavior of the anomalous Green’s function near each S/F interface, assuming that the ferromagnetic interlayer is infinite. This analytical calculation for an S/F/S trilayer with long ferromagnetic interlayer is performed in the next section.

The general expression for the supercurrent is given by

$$J_s = \frac{i\pi T \sigma_n}{4e} \sum_{n=-\infty, \sigma=\uparrow, \downarrow}^{+\infty} \left(\tilde{F}_{f\sigma} \frac{\partial}{\partial x} F_{f\sigma} - F_{f\sigma} \frac{\partial}{\partial x} \tilde{F}_{f\sigma} \right), \quad (9)$$

where $\tilde{F}_{f\uparrow(\downarrow)}(x, \omega) = F_{f\uparrow(\downarrow)}^*(x, -\omega)$ are the anomalous Green’s functions in the ferromagnet.

III. CRITICAL CURRENT OF JUNCTIONS WITH LONG FERROMAGNETIC INTERLAYER

We need to solve the complete nonlinear Usadel equations in the ferromagnet [Eq. (1)]. For SIFS junctions, an analyti-

cal solution may be found if $d_f \gg \xi_{f1}$ and we can set the phase of the anomalous Green's function to zero (see discussion in Sec. II).

Setting $\chi_s = \chi_f = 0$, we have the following θ parametrizations of the normal and anomalous Green's functions [Eq. (8)], $G = \cos \theta$ and $F = \sin \theta$. In this case, we can write Eq. (1) in the F layer as

$$\frac{D_f}{2} \frac{\partial^2 \theta_{f\uparrow(\downarrow)}}{\partial x^2} = \left(\omega \pm ih + \frac{\cos \theta_{f\uparrow(\downarrow)}}{\tau_m} \right) \sin \theta_{f\uparrow(\downarrow)}. \quad (10)$$

In the S layer, the Usadel equation [Eq. (2)] may be now written as

$$\frac{D_s}{2} \frac{\partial^2 \theta_s}{\partial x^2} = \omega \sin \theta_s - \Delta(x) \cos \theta_s. \quad (11)$$

The self-consistency equation in the S layer acquires the form

$$\Delta(x) \ln \frac{T_c}{T} = \pi T \sum_{\omega > 0} \left(\frac{2\Delta(x)}{\omega} - \sin \theta_{s\uparrow} - \sin \theta_{s\downarrow} \right). \quad (12)$$

In the case of $\chi_s = \chi_f = 0$, the boundary conditions [Eqs. (6a)–(6c)] for the functions $\theta_{f,s}$ at each S/F interface can be written as

$$\xi_n \gamma \left(\frac{\partial \theta_f}{\partial x} \right)_{\pm d_f/2} = \xi_s \left(\frac{\partial \theta_s}{\partial x} \right)_{\pm d_f/2}, \quad (13a)$$

$$\xi_n \gamma_{B1} \left(\frac{\partial \theta_f}{\partial x} \right)_{-d_f/2} = \sin(\theta_f - \theta_s)_{-d_f/2}, \quad (13b)$$

$$\xi_n \gamma_{B2} \left(\frac{\partial \theta_f}{\partial x} \right)_{d_f/2} = \sin(\theta_s - \theta_f)_{d_f/2}. \quad (13c)$$

The boundary conditions at $x = \pm \infty$ are

$$\theta_s(\pm \infty) = \arctan \frac{|\Delta|}{\omega}. \quad (14)$$

In the equation for the supercurrent [Eq. (9)], the summation goes over all Matsubara frequencies. It is possible to rewrite the sum only over positive Matsubara frequencies due to the symmetry relation

$$\theta_{f(s)\uparrow}(\omega) = \theta_{f(s)\downarrow}(-\omega). \quad (15)$$

In what follows, we will use only $\omega > 0$ in equations containing ω .

For the left interface (tunnel barrier at $x = -d_f/2$), a first integral of Eq. (10) leads to

$$\frac{\xi_f}{2} \frac{\partial \theta_f}{\partial x} = -q \sin \frac{\theta_f}{2} \sqrt{1 - \epsilon^2 \sin^2 \frac{\theta_f}{2}}, \quad (16)$$

where $\xi_f = \sqrt{D_f/h}$ and the boundary condition $\theta_f(x \rightarrow \infty) = 0$ has been used. In Eq. (16), we use the following notations:

$$q = \sqrt{2/h} \sqrt{\omega \pm ih + 1/\tau_m}, \quad (17a)$$

$$\epsilon^2 = (1/\tau_m)(\omega \pm ih + 1/\tau_m)^{-1}. \quad (17b)$$

Here, we again adopt convention that positive sign ahead of h corresponds to the spin up state (\uparrow) and negative sign to the spin down state (\downarrow). Here and below, we did not write spin labels $\uparrow(\downarrow)$ explicitly but imply them everywhere they needed.

For the right interface ($x = d_f/2$), a first integral of Eq. (10) leads to a similar equation,

$$\frac{\xi_f}{2} \frac{\partial \theta_f}{\partial x} = q \sin \frac{\theta_f}{2} \sqrt{1 - \epsilon^2 \sin^2 \frac{\theta_f}{2}}. \quad (18)$$

Following Faure *et al.*,²⁵ we integrate Eq. (16), which gives

$$\frac{\sqrt{1 - \epsilon^2 \sin^2 \frac{\theta_f}{2}} - \cos \frac{\theta_f}{2}}{\sqrt{1 - \epsilon^2 \sin^2 \frac{\theta_f}{2}} + \cos \frac{\theta_f}{2}} = g_1 \exp\left(-2q \frac{d_f/2 + x}{\xi_f}\right). \quad (19)$$

The integration constant g_1 in Eq. (19) should be determined from the boundary condition at the left S/F interface [Eq. (13b)]. Since we consider the tunnel limit ($\gamma_{B1} \gg 1$), we can neglect small θ_f in the right hand side of Eq. (13b) and also assume, neglecting the inverse proximity effect,

$$\theta_s(-d_f/2) = \arctan \frac{|\Delta|}{\omega}. \quad (20)$$

Then, Eq. (13b) becomes

$$\xi_n \gamma_{B1} \left(\frac{\partial \theta_f}{\partial x} \right)_{-d_f/2} = -G(n), \quad G(n) = \frac{|\Delta|}{\sqrt{\omega^2 + |\Delta|^2}}. \quad (21)$$

From Eqs. (16) and (21), we obtain the boundary value of θ_f at $x = -d_f/2$ and substituting it into Eq. (19), we finally get

$$g_1 = \frac{G^2(n)}{16\gamma_{B1}^2} \frac{1 - \epsilon^2 \left(\frac{\xi_f}{\xi_n}\right)^2}{q^2}. \quad (22)$$

Linearizing Eq. (19), we can now obtain the anomalous Green's function in the ferromagnetic layer of the SIF tunnel junction with infinite F layer thickness. Similar formula for the FS bilayer with a transparent interface ($\gamma_{B2} = 0$) was developed by Faure *et al.*²⁵ [to obtain it one should integrate Eq. (18) and then linearize the resulting equation]. The anomalous Green's function at the center of the F layer in a SIFS junction may be taken as the superposition of the two decaying functions, taking into account the phase difference in each superconducting electrode,

$$\theta_f = \frac{4}{\sqrt{1 - \epsilon^2}} \left[\sqrt{g_1} \exp\left(-q \frac{d_f/2 + x}{\xi_f} - i \frac{\varphi}{2}\right) + \sqrt{g_2} \exp\left(q \frac{x - d_f/2}{\xi_f} + i \frac{\varphi}{2}\right) \right]. \quad (23)$$

The expression for g_2 was obtained in Ref. 25 for the rigid boundary conditions at the transparent FS interface, $\theta_f(d_f/2) = \arctan(|\Delta|/\omega)$ and reads

$$g_2 = \frac{(1 - \epsilon^2)F^2(n)}{[\sqrt{(1 - \epsilon^2)F^2(n) + 1} + 1]^2}, \quad (24a)$$

$$F(n) = \frac{|\Delta|}{\omega + \sqrt{\omega^2 + |\Delta|^2}}. \quad (24b)$$

Using the above solutions and Eqs. (9) and (15), we arrive at sinusoidal current-phase relation in a SIFS tunnel Josephson junction with the critical current

$$I_c R_N = \frac{16\pi T}{e} \operatorname{Re} \left[\sum_{n=0}^{\infty} \frac{G(n)F(n)\exp(-qd_f/\xi_f)}{\sqrt{(1 - \epsilon^2)F^2(n) + 1} + 1} \right]. \quad (25)$$

Here and below, we fix positive sign in the definition of q and ϵ^2 in Eqs. (17a) and (17b): $q = \sqrt{2/h}\sqrt{\omega + ih + 1/\tau_m}$ and $\epsilon^2 = (1/\tau_m)(\omega + ih + 1/\tau_m)^{-1}$. It is possible since we already performed summation over spin states and have to define now spin-independent values. In Eq. (25) and below, R_N is a full resistance of an S/F/S trilayer, which include both interface resistances of left and right interfaces and the resistance of the ferromagnetic interlayer. In case of SIFS and SIFIS junctions, the F layer resistance can be neglected compared to large resistance of the tunnel barrier.

At this point, we define the characteristic lengths of the decay and oscillations $\xi_{f1,2}$ as

$$q/\xi_f = 1/\xi_{f1} + i/\xi_{f2}, \quad (26a)$$

$$\frac{1}{\xi_{f1,2}} = \frac{1}{\xi_f} \sqrt{\sqrt{1 + \left(\frac{\omega}{h} + \frac{1}{h\tau_m}\right)^2} \pm \left(\frac{\omega}{h} + \frac{1}{h\tau_m}\right)}. \quad (26b)$$

The critical current in Eq. (25) is proportional to the small exponent $\exp(-d_f/\xi_{f1})$. The terms neglected in our approach are of the order of $\exp(-2d_f/\xi_{f1})$ and they give a tiny second-harmonic term in the current-phase relation.

The critical current equation [Eq. (25)] can be simplified in the limit of vanishing magnetic scattering, $\tau_m^{-1} \ll \pi T_c$,

$$I_c R_N = \frac{16\pi T}{e} \sum_{n=0}^{\infty} \left[\frac{G(n)F(n)\exp\left(\frac{-d_f}{\xi_{f1}}\right)\cos\left(\frac{d_f}{\xi_{f2}}\right)}{\sqrt{F^2(n) + 1} + 1} \right]. \quad (27)$$

Equation (25) also simplifies near T_c and may be written as (for $T_c \ll h$)

$$I_c R_N = \frac{\pi|\Delta|^2}{2eT_c} \exp\left(-\frac{d_f}{\xi_{f1}}\right)\cos\left(\frac{d_f}{\xi_{f2}}\right). \quad (28)$$

The damped oscillatory behavior of the critical current can be clearly seen from this equation. With increasing d_f , the junction undergoes the sequence of $0-\pi$ transitions when positive values of the $I_c R_N$ product correspond to a zero state and negative values correspond to a π state.

Equation (28) in the absence of spin-flip scattering coincides with the corresponding equation [Eq. (37)] from Ref. 17, taken in the limit of long $d_f \gg \xi_{f1}$ in case of $\gamma_{B1} \gg 1$, $\gamma_{B2} = 0$.

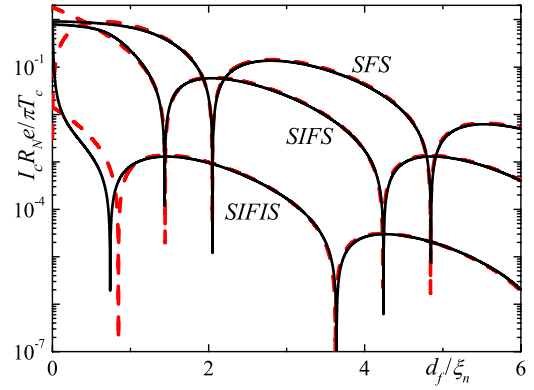


FIG. 2. (Color online) The F layer thickness dependence of the critical current for SFS ($\gamma_{B1,2}=0$), SIFS ($\gamma_{B1}=10^2$, $\gamma_{B2}=0$), and SIFIS ($\gamma_{B1,2}=10^2$) junctions in the absence of spin-flip scattering. Red dashed lines correspond to the modulus of the analytical results [Eqs. (31), (25), and (29)] and black solid lines correspond to the results of numerical calculation in Sec. IV, $h=3\pi T_c$, and $T=0.5T_c$.

Using the same approach, we can obtain the equation for the critical current in a SIFIS structure with two strong tunnel barriers between the ferromagnet and both superconducting layers ($\gamma_{B1,2} \gg 1$),

$$I_c R_N = \frac{4\pi T \xi_f \gamma_{B1} + \gamma_{B2}}{e \xi_n \gamma_{B1} \gamma_{B2}} \operatorname{Re} \left[\sum_{n=0}^{\infty} \frac{G^2(n)\exp\left(\frac{-qd_f}{\xi_f}\right)}{q} \right]. \quad (29)$$

This formula coincides with corresponding expression [Eq. (39)] for the critical current in a SIFIS structure in Ref. 25 for $\gamma_{B1,2} = \gamma_B \gg 1$ and $d_f \gg \xi_{f1}$. Equation (29) near T_c may be written as (for $T_c \ll h$)

$$I_c R_N = \frac{\pi|\Delta|^2 \xi_{f2} \gamma_{B1} + \gamma_{B2}}{2eT_c \xi_n \gamma_{B1} \gamma_{B2}} \cos(\Psi) \exp\left(\frac{-d_f}{\xi_{f1}}\right) \sin\left(\Psi - \frac{d_f}{\xi_{f2}}\right), \quad (30)$$

where Ψ is defined by $\tan(\Psi) = \xi_{f2}/\xi_{f1}$. Equation (30) in the absence of spin-flip scattering coincides with the corresponding equation [Eq. (35)] from Ref. 17, taken in the limit of long $d_f \gg \xi_{f1}$.

We also provide here equation for the critical current in an SFS junction [see Ref. 25, Eq. (74)], written in our notations,

$$I_c R_N = \frac{64\pi T d_f}{e \xi_f} \operatorname{Re} \left[\sum_{n=0}^{\infty} \frac{F^2(n)q \exp(-qd_f/\xi_f)}{[\sqrt{(1 - \epsilon^2)F^2(n) + 1} + 1]^2} \right]. \quad (31)$$

We compare critical current dependencies over d_f for SFS [Eq. (31)], SIFS [Eq. (25)], and SIFIS [Eq. (29)] structures in Fig. 2. Each of above junction types undergoes the sequence of $0-\pi$ transitions with increasing thickness of the F layer. From the figure, we see that the transition from 0 to π state occurs in SIFS tunnel junctions at shorter d_f than in SFS junctions with transparent interfaces, but at longer d_f than in SIFIS junctions with two strong tunnel barriers. This tendency can be qualitatively explained by the fact that in struc-

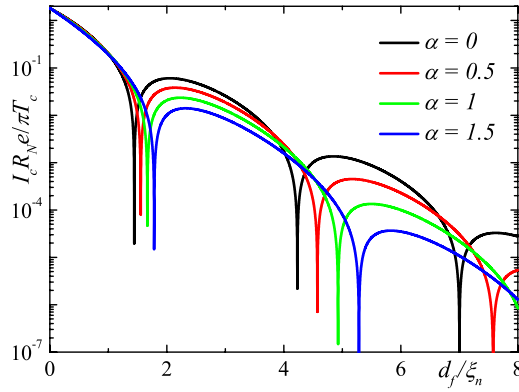


FIG. 3. (Color online) The F layer thickness dependence of the critical current in a SIFS junction [modulus of the Eq. (25)] for different values of $\alpha = 1/\pi T_c \tau_m$, $h = 3\pi T_c$, and $T = 0.5T_c$.

tures with barriers (SIFS, SIFIS) part of the π phase shift occurs across the barriers. Therefore, a thinner F layer in a SIFS junction compared to an SFS one is needed to provide the total shift of π due to the order parameter oscillation. For the same reason, $0-\pi$ transition in a SIFIS junction occurs at a smaller thickness than in a SIFS junction. We note that in Fig. 2, we plot both analytical and numerical calculated $I_c(d_f)$ dependencies, where numerical calculation was performed for full boundary problem [Eqs. (1)–(7)] (see further discussion in Sec. IV).

In Fig. 3, we plot the F layer thickness dependence of the critical current in a SIFS junction for different values of spin-flip scattering time. For stronger spin-flip scattering, the period of supercurrent oscillations increases and the point of $0-\pi$ transition shifts to the region of larger d_f . The same tendency exists for SFS and SIFIS junctions.²⁵

In Fig. 4, we plot the F layer thickness dependence of the critical current in a SIFS junction for different values of the exchange field h . We see that for large exchange fields $h \gg \pi T_c$, the critical current scales with the ferromagnetic coherence length ξ_f .

From comparison with numerical results presented in Fig. 2, we can conclude that the results for the critical current in

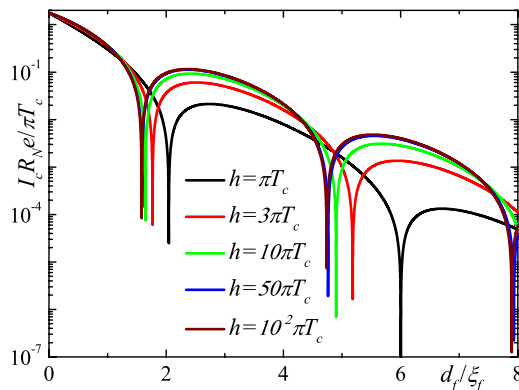


FIG. 4. (Color online) The F layer thickness dependence of the critical current in a SIFS junction [modulus of the Eq. (25)] for different values of exchange field h in the absence of spin-flip scattering, $T = 0.5T_c$.

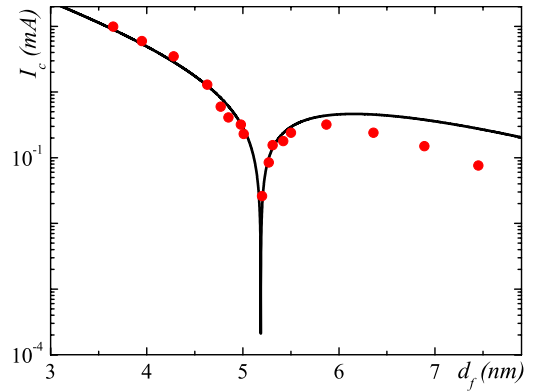


FIG. 5. (Color online) Fit to the experimental data from Ref. 14 for the critical current in a Nb/Al₂O₃/Ni_{0.6}Cu_{0.4}/Nb junction. The fitting parameters are $h/k_B = 950$ K and $1/\tau_m = 1.6$ h.

SIFS junctions presented in Figs. 3 and 4 give correct magnitude of the $I_c R_N$ product for $d_f \gg \xi_n/2$.

As an application of the developed formalism, we present in Fig. 5 the theoretical fit of the experimental data for a Nb/Al₂O₃/Ni_{0.6}Cu_{0.4}/Nb junctions by Weides *et al.*¹⁴ making use of Eq. (25). We used following values of parameters: $R_B = 3.9$ m Ω , $D_f = 3.9$ cm²/s, $T = 4.2$ K,¹⁴ and $T_c = 7.2$ K (damped critical temperature in Nb). Good agreement was obtained with the following parameters: $h/k_B = 950$ K and $1/\tau_m = 1.6$ h (see Fig. 5). These parameters can be compared with parameters obtained by Oboznov *et al.*¹³ for similar ferromagnetic material, Ni_{0.53}Cu_{0.47}: $h/k_B = 850$ K and $1/\tau_m = 1.3$ h. Higher Ni concentration in the NiCu alloy in the experiment of Weides *et al.* results in higher exchange field.

In Ref. 13, it was suggested that a “dead” layer exists in the ferromagnet near each S/F interface, which does not take part in the “oscillating” superconductivity. Other authors also include into consideration the existence of nonmagnetic layers at the interface of the ferromagnet and the superconductor or normal metal.^{26,27,32} Thickness of the dead layer cannot be calculated quantitatively in the framework of our model and also cannot be directly estimated from the experiment. In the experiment of Weides *et al.*,¹⁴ the range of F layer thicknesses was rather narrow and only the first $0-\pi$ transition was observed. Due to these reasons, we did not take into account the existence of a nonmagnetic layer in our fit. This question deserves separate detail experimental and theoretical study.

We should mention that the above estimates of exchange field and spin-flip scattering time could be different if we consider magnetically active S/F interfaces. It was shown in Ref. 28 that the effect of spin-dependent boundary conditions on the superconducting proximity effect in a diffusive ferromagnet results in the change of the period of critical current oscillations.

IV. CRITICAL CURRENT OF JUNCTIONS WITH ARBITRARY LENGTH OF THE FERROMAGNETIC INTERLAYER

In the previous section, we derived the expression for the critical current of a SIFS junction in case of considerably

long F layer thickness, $d_f \gg \xi_{f1}$. For arbitrary F layer thickness in the absence of spin-flip scattering, general boundary problem [Eqs. (1)–(7)] was solved numerically using the iterative procedure.²⁹ Starting from trial values of the complex pair potential $\Delta(x)$ and the Green's functions $\hat{G}_{s,f}$, we solve the resulting boundary problem. After this, we recalculate $\hat{G}_{s,f}$ and $\Delta(x)$. We repeat the iterations until convergency is reached. The self-consistency of calculations is checked by the condition of conservation of the supercurrent across the junction.

In Fig. 2, we compare numerically and analytically calculated $I_c(d_f)$ dependencies in case of SFS, SIFS, and SIFIS junctions. We see that, as expected, the numerical method provides correction only for small length of ferromagnetic layer. We note that for SFS and SIFS junctions, analytical curves [Eq. (31) and (25)] practically coincide with numerical results in the region of the first $0-\pi$ transition. For a SIFIS junction, this transition occurs at smaller d_f , where the assumptions of Sec. III are not valid. However, in the presence of strong spin-flip scattering the first $0-\pi$ transition peak in a SIFIS junction shifts to the region of larger d_f and Eq. (29) describes the transition accurately.

The main result of this section is that Eq. (25) for the critical current of a SIFS junction can be used as a tool to fit experimental data in SIFS junctions with good accuracy.

V. DENSITY OF STATES OSCILLATIONS IN THE FERROMAGNETIC INTERLAYER

It is known that in a ferromagnetic metal attached to the superconductor the quasiparticle DOS at energies close to the Fermi energy has a damped oscillatory behavior.^{33–35} Experimental evidence for such behavior was provided by Kontos *et al.*³⁶ In SIFS junctions, we can compare the DOS oscillations with the critical current oscillations.

We are interested in the quasiparticle DOS in the F layer in the vicinity of the tunnel barrier ($x = -d_f/2 + 0$ in Fig. 1). Below, we will refer to the local DOS at this point. For the case of strong tunnel barrier ($\gamma_{BI} \gg 1$), left S layer and right FS bilayer in Fig. 1 are uncoupled. Therefore, we need to calculate the DOS in the FS bilayer at the free boundary of the ferromagnet. Solving numerically Eqs. (10)–(14), we set to zero the θ_f derivative at the free edge of the FS bilayer, $x = -d_f/2$, $(\partial\theta_f/\partial x)_{-d_f/2} = 0$.³¹

We use the self-consistent two step iterative procedure.^{29–31} In the first step, we calculate the pair potential coordinate dependence $\Delta(x)$ using the self-consistency equation in the S layer [Eq. (12)]. Then, by proceeding to the analytical continuation in Eqs. (10) and (11) over the quasiparticle energy $i\omega \rightarrow E + i0$ and using the $\Delta(x)$ dependence obtained in the previous step, we find the Green's functions by repeating the iterations until convergency is reached. We define the full DOS $N(E)$ and the spin resolved DOS $N_{\uparrow(\downarrow)}(E)$, normalized to the DOS in the normal state, as

$$N(E) = [N_{\uparrow}(E) + N_{\downarrow}(E)]/2, \quad (32a)$$

$$N_{\uparrow(\downarrow)}(E) = \text{Re}[\cos \theta_{\uparrow(\downarrow)}(i\omega \rightarrow E + i0)]. \quad (32b)$$

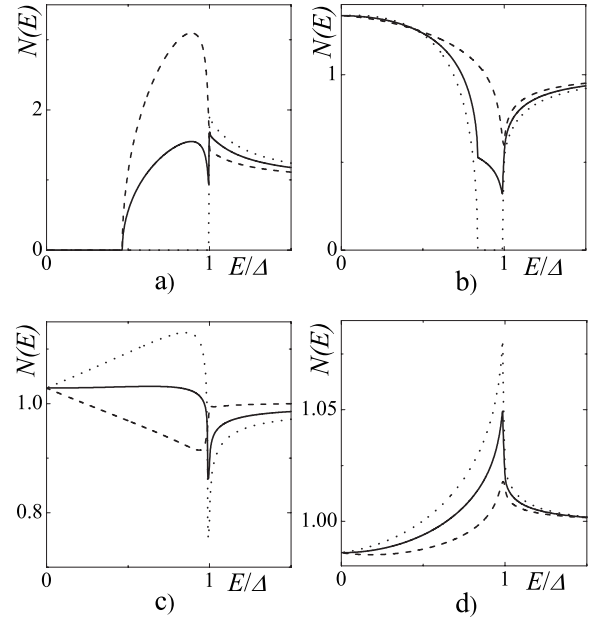


FIG. 6. DOS on the free boundary of the F layer in the FS bilayer calculated numerically in the absence of spin-flip scattering for different values of the F layer thickness d_f : $N_{\uparrow}(E)$ (dashed line), $N_{\downarrow}(E)$ (dotted line), and $N(E)$ (solid line), $E_{ex} = 3\pi T_c$, and $T = 0.5T_c$. (a) $d_f/\xi_n = 0.4$, (b) $d_f/\xi_n = 1$, (c) $d_f/\xi_n = 1.6$, and (d) $d_f/\xi_n = 2.2$.

The numerically obtained energy dependencies of the DOS at the free F boundary of the FS bilayer are presented in Figs. 6 and 7. Figure 6 demonstrates the DOS energy dependence for different d_f . At small d_f , full DOS turns to zero

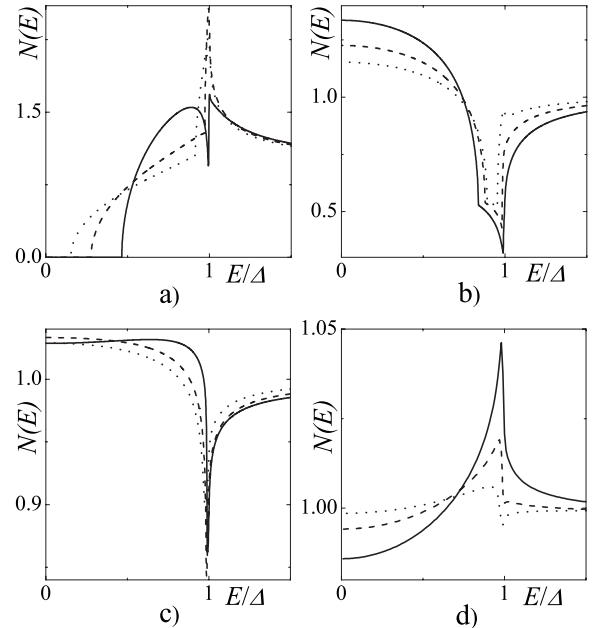


FIG. 7. DOS $N(E)$ on the free boundary of the F layer in the FS bilayer calculated numerically for $\alpha = 1/\pi T_c \tau_m = 0$ (solid line), $\alpha = 0.5$ (dashed line), and $\alpha = 1$ (dotted line) for different values of the F layer thickness d_f , $E_{ex} = 3\pi T_c$, and $T = 0.5T_c$. (a) $d_f/\xi_n = 0.4$, (b) $d_f/\xi_n = 1$, (c) $d_f/\xi_n = 1.6$, and (d) $d_f/\xi_n = 2.2$.

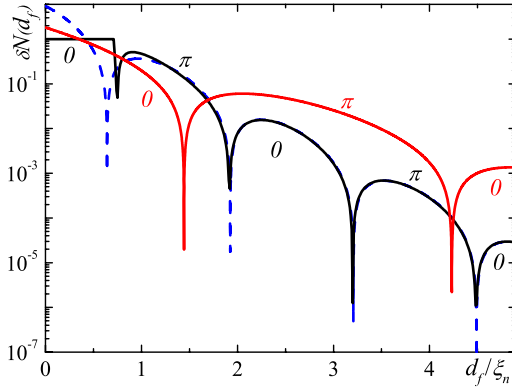


FIG. 8. (Color online) The F-layer dependence of the function $\delta N(d_f)$ in the absence of spin-flip scattering, $h=3\pi T_c$, $T=0.5T_c$. Black solid line is a result of the numerical calculation; blue dashed line is calculated with the use of Eq. (41). Red line shows normalized critical current for a SIFS junction. Zero and π states defined from I_c are indicated by red color, while zero and π states defined from the DOS are indicated by black color.

inside a minigap, which vanishes with the increase of d_f . Then, the DOS at the Fermi energy $N(0)$ rapidly increases to the values larger than unity and with further increase of d_f it oscillates around unity, while its absolute value exponentially approaches unity (see also Fig. 8). In Fig. 6, we also plot the spin resolved DOS energy dependencies $N_{\uparrow}(E)$ and $N_{\downarrow}(E)$. Figure 7 demonstrates full DOS energy dependence for different values of spin-flip scattering time. For stronger spin-flip scattering, the minigap closes at smaller d_f , the period of the DOS oscillations at the Fermi energy increases, and the damped exponential decay occurs faster.

In case of long F layer ($d_f \gg \xi_f$) it is also possible to obtain an analytical expression for the DOS at the free boundary of the ferromagnet,

$$N_{\uparrow(\downarrow)}(E) = \text{Re}[\cos \theta_{b\uparrow(\downarrow)}] \approx 1 - \frac{1}{2} \text{Re} \theta_{b\uparrow(\downarrow)}^2, \quad (33)$$

where $\theta_{b\uparrow(\downarrow)}$ is a boundary value of θ_f at $x=-d_f/2$. It can be obtained by the mapping method, similar to the one used in the electrostatic problems. We consider the FS bilayer where $x \in [-d_f/2, d_f/2]$ stands for the ferromagnetic metal and $x > d_f/2$ stands for the superconductor; the point $x=-d_f/2$ corresponds to the free F layer boundary. For infinite F layer ($d_f \rightarrow \infty$), the solution for $\theta_{f\uparrow(\downarrow)}$ far from the interface is given by the exponential term in Eq. (23), written in the real energy space,

$$\tilde{\theta}_{f\uparrow(\downarrow)} = \frac{4}{\sqrt{1-\eta^2}} \sqrt{g_2} \exp\left(p \frac{x-d_f/2}{\xi_f}\right), \quad (34)$$

where

$$p = \sqrt{2/h} \sqrt{-iE_R \pm ih + 1/\tau_m}, \quad (35a)$$

$$\eta^2 = (1/\tau_m)(-iE_R \pm ih + 1/\tau_m)^{-1}, \quad (35b)$$

$$g_2 = \frac{(1-\eta^2)F^2(E)}{[\sqrt{(1-\eta^2)F^2(E)+1+1}]^2}, \quad (35c)$$

$$F(E) = \frac{|\Delta|}{-iE_R + \sqrt{|\Delta|^2 - E_R^2}}, \quad E_R = E + i0. \quad (35d)$$

Here, as above, positive sign ahead of h corresponds to the spin up state in Eq. (34) and negative sign for the spin down state. By using the arrow “from right to left” in $\tilde{\theta}_{f\uparrow(\downarrow)}$, we want to stress that this solution is induced in the ferromagnet from the right FS interface.

In the case of finite ferromagnet length, the boundary conditions at the free F layer boundary, $x=-d_f/2$, become

$$\theta_{f\uparrow(\downarrow)}(-d_f/2) = \theta_{b\uparrow(\downarrow)}, \quad \left(\frac{\partial \theta_{f\uparrow(\downarrow)}}{\partial x}\right)_{-d_f/2} = 0. \quad (36)$$

To ensure these conditions, we add another exponential solution,

$$\tilde{\theta}_{f\uparrow(\downarrow)} = \frac{4}{\sqrt{1-\eta^2}} \sqrt{g_2} \exp\left(-p \frac{3d_f/2+x}{\xi_f}\right), \quad (37)$$

resulting from the mirror image of the F layer with respect to the point $x=-d_f/2$. At $x=-d_f/2$ both exponential terms are equal to each other and the final solution, $\theta_{b\uparrow(\downarrow)} = \tilde{\theta}_{f\uparrow(\downarrow)}(-d_f/2) + \tilde{\theta}_{f\uparrow(\downarrow)}(-d_f/2)$, is two times larger than the solution for infinite ferromagnetic layer at this point and reads

$$\theta_{b\uparrow(\downarrow)} = \frac{8F(E)}{\sqrt{(1-\eta^2)F^2(E)+1+1}} \exp\left(-p \frac{d_f}{\xi_f}\right). \quad (38)$$

This equation coincides with the result obtained in Ref. 32 by direct integration of the Usadel equation.

In Fig. 8, we plot analytically and numerically calculated function

$$\delta N(d_f) = |1 - N_0|, \quad N_0 = N(E=0), \quad (39)$$

together with the $I_c(d_f)$ dependence for a SIFS junction. We see that the point of 0- π transition on the $I_c(d_f)$ plot does not coincide with the first minimum of $\delta N(d_f)$ corresponding to sign change of $1-N_0$. This difference can be qualitatively explained as follows. The transition from 0 to π state in a junction, seen as sign change of $I_c(d_f)$, is the result of interference of solutions for θ_f originating from two S electrodes. 0- π transition in $I_c(d_f)$ occurs approximately at such thickness d_f when the boundary value of θ_f in Eq. (23) at $x=-d_f/2$ becomes negative, i.e., when θ_f acquires the phase shift π . On the other hand, sign change of $1-N_0$ occurs at such d_f when the boundary value θ_b in Eq. (38) becomes an imaginary number, i.e., when θ_f acquires the phase shift $\pi/2$. It occurs at smaller d_f compared to 0- π transition in the critical current. Corresponding 0 and π states defined from I_c and from the DOS are indicated in Fig. 8.

It is also seen from Fig. 8 that the DOS oscillations have the period approximately twice smaller than those of the critical current. This fact is easy to see from the analytical expression for $\delta N(d_f)$. Using Eqs. (32)–(39), we obtain

$$\delta N(d_f) = 32 \left| \operatorname{Re} \left[\frac{1}{(\sqrt{2 - \eta_0^2} + 1)^2} \exp \left(-p_0 \frac{2d_f}{\xi_f} \right) \right] \right|, \quad (40)$$

where $\eta_0 = \eta(E=0)$ and $p_0 = p(E=0)$ in Eqs. (35a) and (35b). At vanishing magnetic scattering, $\tau_m^{-1} \ll \pi T_C$, this equation can be simplified,

$$\delta N(d_f) = \frac{32}{3 + 2\sqrt{2}} \left| \exp \left(-\frac{2d_f}{\xi_{f1}} \right) \cos \left(\frac{2d_f}{\xi_{f2}} \right) \right|, \quad (41)$$

where characteristic lengths of decay and oscillations $\xi_{f1,2}$ are given by Eq. (26b) with the substitution $i\omega \rightarrow E + i0$. This equation can be compared with Eq. (27). We see that the period of the DOS oscillations is approximately twice smaller than the period of the critical current oscillations and the exponential decay is approximately twice faster than the decay of the critical current.

VI. CONCLUSION

We have developed a quantitative model, which describes the oscillations of the critical current as a function of the F layer thickness in an SIFS tunnel junctions with thick ferromagnetic interlayer, $d_f \gg \xi_{f1}$, in the dirty limit. We justified this model by numerical calculations in general case of arbitrary d_f : for all values of parameters characterizing material

properties of the ferromagnetic metal numerical and analytical results coincide in physically important region of the first $0-\pi$ transition. Thus, the derived analytical expression for the critical current can be used as a tool to fit experimental data in various types of SIFS junctions. We have discussed the details of the damped oscillatory behavior of the critical current for different values of the F layer parameters.

We also studied the superconducting DOS induced in a ferromagnet by the proximity effect. We showed that the oscillation pattern of DOS at the Fermi energy in the ferromagnet (at location of the tunnel junction) does not coincide with that of the critical current in a SIFS junction and its period is approximately twice smaller. Therefore, the DOS oscillations do not reflect the $0-\pi$ transition in $I_c(d_f)$. We calculated the quasiparticle DOS in the F layer in the close vicinity of the tunnel barrier which can be used to obtain current-voltage characteristics for a SIFS junction. These calculations will be presented elsewhere.

Finally, we used our results to fit recent experimental data for SIFS tunnel junctions and extracted important parameters of the ferromagnetic interlayer.

ACKNOWLEDGMENTS

The authors thank W. Belzig, E. V. Bezuglyi, A. I. Buzdin, T. Champel, S. Kawabata, and F. Pistolesi for useful discussions. This work was supported by NanoNed program under Project No. TCS7029 and RFBR Project No. N08-02-90012.

*Present address: LPMMC, Université Joseph Fourier and CNRS, 25 Avenue des Martyrs, BP 166, 38042 Grenoble, France

¹A. I. Buzdin, *Rev. Mod. Phys.* **77**, 935 (2005).
²A. A. Golubov, M. Yu. Kupriyanov, and E. Il'ichev, *Rev. Mod. Phys.* **76**, 411 (2004).
³F. S. Bergeret, A. F. Volkov, and K. B. Efetov, *Rev. Mod. Phys.* **77**, 1321 (2005).
⁴V. V. Ryazanov, V. A. Oboznov, A. Yu. Rusanov, A. V. Veretennikov, A. A. Golubov, and J. Aarts, *Phys. Rev. Lett.* **86**, 2427 (2001); V. V. Ryazanov, V. A. Oboznov, A. V. Veretennikov, and A. Yu. Rusanov, *ibid.* **65**, 020501(R) (2001).
⁵T. Kontos, M. Aprili, J. Lesueur, F. Genet, B. Stephanidis, and R. Boursier, *Phys. Rev. Lett.* **89**, 137007 (2002).
⁶Y. Blum, A. Tsukernik, M. Karpovski, and A. Palevski, *Phys. Rev. Lett.* **89**, 187004 (2002).
⁷H. Sellier, C. Baraduc, F. Lefloch, and R. Calemczuk, *Phys. Rev. Lett.* **92**, 257005 (2004).
⁸A. Bauer, J. Bentner, M. Aprili, M. L. Della-Rocca, M. Reinwald, W. Wegscheider, and C. Strunk, *Phys. Rev. Lett.* **92**, 217001 (2004).
⁹C. Bell, R. Loloee, G. Burnell, and M. G. Blamire, *Phys. Rev. B* **71**, 180501(R) (2005).
¹⁰F. Born, M. Siegel, E. K. Hollmann, H. Braak, A. A. Golubov, D. Yu. Gusakova, and M. Yu. Kupriyanov, *Phys. Rev. B* **74**, 140501(R) (2006).
¹¹V. Shelukhin, A. Tsukernik, M. Karpovski, Y. Blum, K. B. Efetov, A. F. Volkov, T. Champel, M. Eschrig, T. Lofwander, G.

Schon, and A. Palevski, *Phys. Rev. B* **73**, 174506 (2006).
¹²G. P. Pepe, R. Latempa, L. Parlato, A. Ruotolo, G. Ausanio, G. Peluso, A. Barone, A. A. Golubov, Ya. V. Fominov, and M. Yu. Kupriyanov, *Phys. Rev. B* **73**, 054506 (2006).
¹³V. A. Oboznov, V. V. Bol'ginov, A. K. Feofanov, V. V. Ryazanov, and A. I. Buzdin, *Phys. Rev. Lett.* **96**, 197003 (2006).
¹⁴M. Weides, M. Kemmler, E. Goldobin, D. Koelle, R. Kleiner, H. Kohlstedt, and A. Buzdin, *Appl. Phys. Lett.* **89**, 122511 (2006).
¹⁵M. Weides, M. Kemmler, E. Goldobin, H. Kohlstedt, R. Waser, D. Koelle, and R. Kleiner, *Phys. Rev. Lett.* **97**, 247001 (2006); M. Weides, C. Schindler, and H. Kohlstedt, *J. Appl. Phys.* **101**, 063902 (2007).
¹⁶E. Terzioglu and M. R. Beasley, *IEEE Trans. Appl. Supercond.* **8**, 48 (1998); G. Blatter, V. B. Geshkenbein, and L. B. Ioffe, *Phys. Rev. B* **63**, 174511 (2001); A. V. Ustinov and V. K. Kaplunenko, *J. Appl. Phys.* **94**, 5405 (2003).
¹⁷A. Buzdin and I. Baladie, *Phys. Rev. B* **67**, 184519 (2003).
¹⁸F. S. Bergeret, A. F. Volkov, and K. B. Efetov, *Phys. Rev. B* **64**, 134506 (2001).
¹⁹K. D. Usadel, *Phys. Rev. Lett.* **25**, 507 (1970).
²⁰E. A. Demler, G. B. Arnold, and M. R. Beasley, *Phys. Rev. B* **55**, 15174 (1997).
²¹M. Houzet, V. Vinokur, and F. Pistolesi, *Phys. Rev. B* **72**, 220506(R) (2005).
²²F. S. Bergeret, A. F. Volkov, and K. B. Efetov, *Phys. Rev. B* **75**, 184510 (2007).
²³M. Yu. Kupriyanov and V. F. Lukichev, *Sov. Phys. JETP* **67**,

- 1163 (1988) [Zh. Eksp. Teor. Fiz. **94**, 139 (1988)].
- ²⁴A. D. Zaikin and G. F. Zharkov, Sov. J. Low Temp. Phys. **7**, 184 (1981) [Fiz. Nizk. Temp. **7**, 375 (1981)].
- ²⁵M. Faure, A. I. Buzdin, A. A. Golubov, and M. Yu. Kupriyanov, Phys. Rev. B **73**, 064505 (2006).
- ²⁶A. Ruotolo, C. Bell, C. W. Leung, and M. G. Blamire, J. Appl. Phys. **96**, 512 (2004).
- ²⁷J. Kim, J. H. Kwon, K. Char, H. Doh, and H.-Y. Choi, Phys. Rev. B **72**, 014518 (2005).
- ²⁸A. Cottet and W. Belzig, Phys. Rev. B **72**, 180503(R) (2005).
- ²⁹A. A. Golubov, M. Yu. Kupriyanov, and Ya. V. Fominov, JETP Lett. **75**, 190 (2002) [Pis'ma Zh. Eksp. Teor. Fiz. **75**, 223 (2002)].
- ³⁰A. A. Golubov and M. Yu. Kupriyanov, J. Low Temp. Phys. **70**, 83 (1988); Sov. Phys. JETP **69**, 805 (1989) [Zh. Eksp. Teor. Fiz. **96**, 1420 (1989)]; A. A. Golubov, E. P. Houwman, J. G. Gijsbertsen, V. M. Krasnov, J. Flokstra, H. Rogalla, and M. Yu. Kupriyanov, Phys. Rev. B **51**, 1073 (1995).
- ³¹D. Yu. Gusakova, A. A. Golubov, M. Yu. Kupriyanov, and A. Buzdin, JETP Lett. **83**, 327 (2006) [Pis'ma Zh. Eksp. Teor. Fiz. **83**, 385 (2006)].
- ³²L. Cretinon, A. K. Gupta, H. Sellier, F. Lefloch, M. Faure, A. Buzdin, and H. Courtois, Phys. Rev. B **72**, 024511 (2005).
- ³³A. Buzdin, Phys. Rev. B **62**, 11377 (2000); I. Baladie and A. Buzdin, *ibid.* **64**, 224514 (2001).
- ³⁴M. Zareyan, W. Belzig, and Yu. V. Nazarov, Phys. Rev. Lett. **86**, 308 (2001).
- ³⁵F. S. Bergeret, A. F. Volkov, and K. B. Efetov, Phys. Rev. B **65**, 134505 (2002).
- ³⁶T. Kontos, M. Aprili, J. Lesueur, and X. Grison, Phys. Rev. Lett. **86**, 304 (2001).